Nonlinear Branch-Point Dynamics of Multiarm Polystyrene

Jens Kromann Nielsen,[†] Henrik Koblitz Rasmussen,[‡] Martin Denberg,[†] Kristoffer Almdal,[§] and Ole Hassager*,[†]

The Danish Polymer Centre, Department of Chemical Engineering, Department of Manufacturing Engineering and Management, Technical University of Denmark, DK-2800 Kgs. Lyngby, Denmark, and Risø National Laboratory, DK-4000 Roskilde, Denmark

Received June 30, 2006; Revised Manuscript Received October 6, 2006

ABSTRACT: Two branched polystyrene melts with narrow molar mass distribution have been synthesized: a multiarm $A_n-C-C-A_n$ pom-pom polystyrene and an A_n-C asymmetric star polystyrene where n is the number of arms. The pom-pom and the asymmetric star have molar masses of $M_w = 300$ kg/mol and $M_w = 275$ kg/mol, respectively. The pom-pom was estimated to have 2.5 arms on average, while the estimate is 3.3 for the asymmetric star. The molar mass of each arm is about 27 kg/mol. The melts were characterized in the linear viscoelastic regime and by elongational rheometry in the nonlinear regime. For asymmetric star polystyrene, the measured transient elongational viscosity is not consistent with a rheological constitutive equation that is separable in time and strain. Contrary to this situation, however, for pom-pom polystyrene, the transient elongational viscosity may be described by a time−strain separable constitutive equation for elongation rates larger than the inverse reptation time. Up to a Hencky strains of 2.6, the corresponding stress tensor component for the pom-pom is closely approximated by a model that assumes the arms to be fully relaxed while the cross-bar is part of an unrelaxed entanglement network model. At Hencky strains above 2.6 a saturation of stress occurs that we interpret as withdrawal of the arms into the cross-bar tube. The observed strain associated with arm withdrawal is significantly larger than that predicted from an equilibrium force balance on the branch points while it corresponds well with an estimate of the maximum stretchability of the cross-bar. At the highest elongation rate investigated, the transient elongational viscosity for pom-pom went through a reproducible maximum as a function of time.

1. Introduction

Well-defined branched polymer melts have proven valuable as model materials useful to gain insight into the complex physics of long chain branched (LCB) polymer melts. In one model architecture, often denoted pom-pom polymer, two branch points are connected by a polymer backbone denoted by the cross-bar. A number of arms emanate from the branch points. We refer to the pom-pom as $A_n-C-C-A_n$ and to the asymmetric star as A_n-C. Note that all blocks in the polymers consist of homopolymers. Figure 1 shows a schematic drawing of a pom-pom polystyrene molecule with three arms. In a comprehensive investigation of model branched melts, McLeish and co-workers[1] have reported theory, rheology, and scattering of four isoprene H-shaped polymers (pom-pom polymer with two arms). Archer and Juliani[2] have reported on the dynamics of multiarm $A_n-C-C-A_n$ 1,4-polybutadiene melts. According to the H-polymer theory,[1,3] relaxation in branched systems occurs in a hierarchial fashion: arms relax on a shorter time scale than the cross-bar. The cross-bar does not begin to relax before the arms are completely relaxed, whereby a separation of time scales occurs. Qualitative agreement is generally observed between theory and experiments in the linear viscoelastic regime.[1,2,4]

In the nonlinear range, the additional phenomenon of branch-point withdrawal is believed to occur for large deformations. Once the cross-bar reaches a critical extension, the tension in the cross-bar is sufficient to pull the arms into the cross-bar tube.[5] A force balance on the branch point leads to the prediction[5] that the resulting arm retraction should occur when the relative stretch of the crossbar equals the number of arms. In nonlinear step strain the predicted critical magnitude of strain[6] is approximately $\gamma = \sqrt{3(q^2-1)}$, where q is the number of arms. Archer and Juliani[2] used 3-arm polybutadiene melts[2] to test this prediction up to shear strain magnitudes of 12. They do indeed find a transition at about the predicted critical shear magnitude. However, the measured stress is less than predicted by the theory, especially below the transition point where the material is predicted to behave as an elastomeric network.

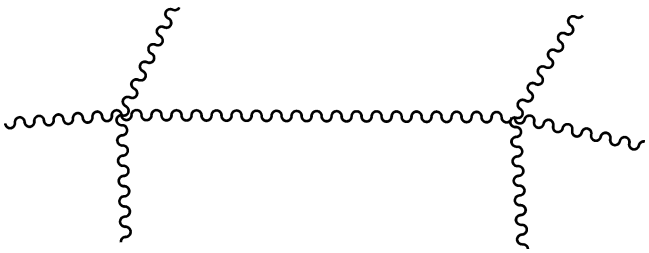

Figure 1. Schematic drawing of a pom-pom molecule with three branches linked to the cross-bar. The chemical formula for the polymer is $(St_m)_n-(St_k)-(St_k)-(St_m)_n$ where St is styrene, n is the number of arms, m is the number of monomers in the arms, and k is half the number of monomers in the cross-bar. We simplify the nomenclature so that the arm is $A \equiv St_m$ and cross-bar is $C \equiv St_k$. The pom-pom is referred to as $A_n-C-C-A_n$ and the asymmetric star as A_n-C.

Experimental information on well-characterized model LCB melts in nonlinear elongation is more limited.[1] Arm retraction has been predicted[6] to cause failure of polymer filaments in extension. Consequently, steady stress will not be observed unless special precautions are made.[7]

In an early development on the rheology of LCB melts, Wagner[8] demonstrated that it is possible to separate time and strain effects in start-up of elongational flow of low-density polyethylene (LDPE) melts. From the resulting strain informa-

[†] Department of Chemical Engineering, Technical University of Denmark.
[‡] Department of Manufacturing Engineering and Management, Technical University of Denmark.
[§] Risø National Laboratory.
* Corresponding author. E-mail: oh@kt.dtu.dk.

10.1021/ma061476r CCC: $33.50
Published on Web 11/16/2006

tion it is then possible to obtain information on the nonlinear strain behavior, including arm retraction in elongation. We intend here to use this methodology to investigate the nonlinear rheology of well-characterized model LCB melts in elongational flow. In particular, we study long-chain branched $A_n-C-C-A_n$, pom-pom, and A_n-C, asymmetric star, polystyrene melts. With a glass transition temperature around 100 °C polystyrene has proven to be a suitable model melt. In the temperature range 130−170 °C we can adjust the time constants of the melt to suit the operating conditions for the rheometer. Time−temperature shifting may then be applied to check consistency of the measurements.

Knauss and Huang[9] developed a metod for preparation of $A_n-C-C-A_n$ polystyrenes by anionic polymerization. The number of arms is not a fixed value but rather a distribution with an average value N_n given by the stoichiometry.[11] In the work by Knauss and Huang and in the more recent work by Ryu et al.[11] all arms are below one entanglement length, however. To be able to compare with H-polymer theory, we have synthesized an $A_n-C-C-A_n$ with about two entanglements in each arm. With this length of the arms the final step in the pom-pom synthesis, the reaction between two asymmetric stars appeared to be a difficult task. However, we used an alternative coupler,[12] 2,2-dimethyl-1,3-ditosylenepropane (DMDSP), that did enable a high yield of the desired $A_n-C-C-A_n$ pom-pom polystyrene. Important for the success of the pom-pom synthesis was also the determination of the rate constant for the anionic polymerization in the presence of THF, whereby the optimal time for addition of the coupler could be computed.

In the elongational flow rheology we use a filament stretching rheometer[13] modified with a thermostat for polymer melts.[14] While elongational rheometers normally require large quantities of the polymer, this instrument operates with samples of about 0.1−0.2 g for a single measurement.

2. Experimental Section

2.1. Materials. Styrene (from Aldrich with purity larger than 99%) was first filtered through a column of aluminum oxide (Aldrich) to remove stabilizer and water. The styrene was vacuum-distilled twice from dibutylmagnesium immediately before use. Living styryl anion was generated in the solvent, cyclohexane (Fisher Scientific, HPLC grade with purity larger than 99.8%), by adding styrene and *sec*-butyllithium (Aldrich, 1.6 M in hexane). Following reflux under argon the cyclohexane was distilled into the reactor. Tetrahydrofuran (THF) (purity larger than 99.5%) from Fisher Scientific was purified by passage through aluminum oxide before it was refluxed under argon in the presence of sodium (Aldrich, 30−35 wt % dispersion in paraffin). 4-(Chlorodimethylsilyl)styrene (CDMSS) was synthesized as reported in ref 9 from *p*-chlorostyrene (Aldrich, purity larger than 97%) and dichlorodimethylsilane (Aldrich) in a Grignard reaction and purified by vacuum distillation prior to use.

2.2. Coupling and Kinetics Experiments. Linear styryl anions were polymerized in a solvent consisting of 97 wt % cyclohexane and 3 wt % THF to a length of about 50 kg/mol at 8 °C. The stoichiometric amount of the bifunctional coupler, dichlorodimethylsilane, was then titrated into the reaction mixture over ~60 min, at which point the mixture changed color from yellow to colorless, indicating that all anions had reacted.

A similar experiment was performed with an alternative bifunctional coupler, DMDSP. The coupling reaction is shown in Figure 2. The coupling reaction with DMDSP was considerably slower than using dichlorodimethylsilane, and the change in color from yellow to colorless took about 24 h. To compare the two coupling agents both polymers were analyzed by size exclusion chromatography (SEC), as shown in Figure 3.

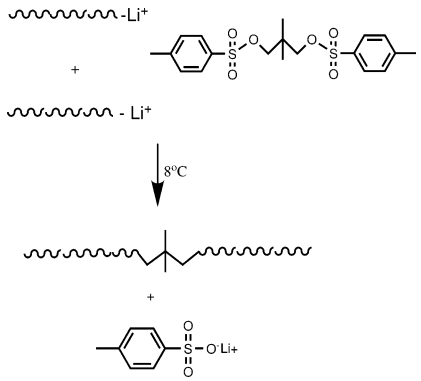

Figure 2. Bifunctional coupling using 2,2-dimethyl-1,3-ditosylenepropane (DMDSP).

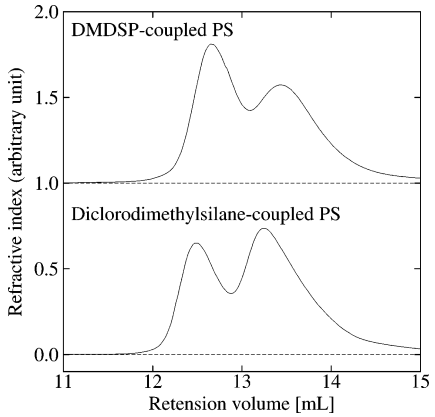

Figure 3. Comparison of SEC output for linear polystyrene obtained from coupling styryl anions with DMDSP and dichlorodimethylsilane, respectively.

Table 1. Experimental Conditions for Determination of Rate Constants for Anionic Polymerization

	temp (°C)	[BuLi] (mol/L)	vol of styrene (mL)	vol of cyclohexane (mL)	vol of THF (mL)
expt 1	3	0.92×10^{-3}	11.21	201.40	6.20
expt 2	8	1.76×10^{-3}	27.97	251.00	7.20

We observed that the styryl anions in the 97% cyclohexane/3% THF solvent even at reduced temperature were less stable than in a 100% cyclohexane solution at room temperature and in fact deactivate after about 3 h, leaving almost no chemically active "asymmetric star" molecules.

To estimate the optimal time and temperature for introduction of the DMDSP coupler further, two model experiments were conducted. Anionic polymerization of linear polystyrene was performed according to the protocol given by Ndoni et al.,[10] substituting the 100% cyclohexane solvent with a 97% cyclohexane/3% THF solvent. In the two experiments we initiated styrene with *sec*-butyllithium at 3 and 8 °C, respectively. During the polymerization a series of exactly 1.00 mL samples were transferred from the reaction mixture to vials containing a toluene/methanol mixture, where methanol acts as a terminating agent for the polymerization. The conversion was determined by measuring the polymer mass concentration (proportional to the integrated differential refractive index (DRI) signal) in these samples. The amounts of chemicals used in the two experiments along with the temperatures used are listed in Table 1.

2.3. Synthesis of the Asymmetric Star. All polymerizations were performed in a round-bottom flask with five necks, thermostated in a water bath. The anionic polymerizations were done in an argon atmosphere under a slight overpressure of 0.2 bar. The first step was to synthesize the linear polystyrene for the arms of the stars. Styrene was dissolved, 5−10 wt %, in cyclohexane, and

a stoichiometric amount of *sec*-butyllithium was added using a gastight syringe. This mixture was left overnight at room temperature under stirring.

In the second ste**p**, the temperature was lowered to 8 °C, and purified THF was added by cannula to reach 3 wt % THF. The stoichiometric amount of CDMSS was then added using a gastight syringe, all at once, and the coupling reaction was left for 1−2 h.

In the third step more styrene monomer was added to make the long arm in the asymmetric star. To terminate the living anion in the "asymmetric star" formation, degassed methanol was added after a reaction time of about 100 min. This reaction time is estimated from an independent kinetics investigation, as explained in section 3.2. The dissolved polymer solutions was then precipitated in 2-propanol and washed with HPLC-grade methanol before being filtered. The reaction mixture was fractionated to remove low molecular weight byproducts. We used toluene/methanol as solvent/nonsolvent pair for fractional precipitation of the highest molar mass polystyrene component.

2.4. Synthesis of the Pom-Pom. The synthesis of the pom-pom followed the same protocol as for the asymmetric star, except instead of terminating with methanol a fourth step was added after the 100 min. In this step, two-thirds of the stoichiometric amount of DMDSP was added and the reaction was left overnight. Then more bifunctional coupler was added slowly until the yellow color from the styryl anion disappeared. The expected coupling scheme is shown in Figure 2.

2.5. Chromatography. The molar mass was determined by size exclusion chromatography (SEC) with THF as the eluent and employing a column set consisting of a 5 μm guard column and two 300 × 8 mm^2 columns (PLgel Mixed C and Mixed D). The system is equipped with a triple detector system, a combined Viscotek model 200 differential diffractive index (DRI) and differential viscosity detector, and a Viscotek model LD 600 right angle laser light scattering detector (RALLS).

The column is calibrated with a number of narrow molar mass distribution linear polystyrene standards. The application of this calibration to the branched pom-pom and asymmetric star may underestimate the molar mass to some extent, depending on the amount of branching. To check the molar mass of the branched polymers, we use a method that is independent of the measured retention time but employs both the DRI and RALLS signals as follows:

$$\mathrm{DRI} = k_1 c \frac{\partial n}{\partial c} \tag{1}$$

$$\mathrm{RALLS} = k_2 c M \left(\frac{\partial n}{\partial c}\right)^2 \tag{2}$$

Here k_1 and k_2 are proportionality constants, c is the mass concentration, and $\partial n/\partial c$ the refractive index increment. These equations may be used to obtain

$$M = \frac{\mathrm{RALLS}(k_1/k_2)}{\mathrm{DRI}(\partial n/\partial c)} \tag{3}$$

This relation is used to compute M from the two signals and a knowledge of $(k_2/k_1)(\partial n/\partial c)$. Since the relation is independent of branching, the quantity $(k_1/k_2)(\partial n/\partial c)$ is determined from the SEC signals of a narrow MMD linear polystyrene standard. We evaluate the signals at the peak value of the RALLS signal to obtain a measurement of the mass average molar mass, M_w, of the pom-pom molecule independent of the column calibration (Table 2).

2.6. Mechanical Spectroscopy. We performed small-amplitude oscillatory shear to obtain an accurate determination of the linear viscoelastic properties (LVE) of the polystyrene melts. We used a plate−plate geometry on an AR2000 rheometer from TA Instruments. The measurements were performed at 130 and 150 °C for both melts and at 140 and 170 °C for the pom-pom molecule. The measured data were time−temperature shifted to master curves at 130 °C using the time−temperature superposition shift factor a_T [15] found from the WLF equation:[16]

$$\log(a_T) = \frac{-c_1^0(T - T_0)}{c_2^0 + (T - T_0)} \tag{4}$$

where the reference temperature $T_0 = 136.5$ °C and the parameters $c_1^0 = 8.86$ and $c_2^0 = 101.6$ °C. T is the sample temperature in °C.

Table 2. Chemical and Physical (130 °C) Properties of Model Polymers[a]

	pom-pom	asymmetric star	linear
A_n, $n \approx$	2.5	3.3	
M_w (eq 3)	300 kg/mol	not measured	not measured
M_w (linear)	280 kg/mol	275 kg/mol	390 kg/mol
M_w/M_n	1.08	1.08	1.06
$M_{n,A}$	28 kg/mol	25 kg/mol	
$M_{w,A}/M_{n,A}$	1.06	1.05	
$M_{n,B} \approx$	140 kg/mol	170 kg/mol	
n_e	0.10	0.10	0.16
n_g	0.67	0.67	0.7
λ_c	0.4 s	0.4 s	0.4 s
G_N^0	480 kPa	540 kPa	257 kPa
$G_{N,1}^0$	120 kPa	250 kPa	257 kPa
$G_{N,2}^0$	360 kPa	290 kPa	
$\lambda_{max,1}$	11000 s	14000 s	21000 s
$\lambda_{max,2}$	70 s	56 s	
$\lambda_{a,1}$	5760 s	7330 s	11270 s
$\lambda_{a,2}$	37 s	29 s	

[a] The third column contain data for a narrow MMD linear polystyrene melt.[16] N_n indicates the number of arms (pom-pom and asymmetric star). M_w (linear) is obtained from a column calibrated with linear standards; M_w (eq 3) is obtained by a technique independent of column calibration (pom-pom only).

2.7. Filament Stretching Rheometer. We used a filament stretching rheometer in which the sample is surrounded by a thermostated environment. This chamber contains a nitrogen gas atmosphere during the extension of the polystyrene samples.

The procedure designed to prepare the cylindrical polystyrene sample, with radius of $R_i = 4.5$ mm and height of $L_i = 2.0$ mm, and apply these to the cylindrical-shaped stainless steel end plates is described in detail in Bach et al.[14] In all of the experiments the sample was prestretched (at 150 °C) to reduce the transmitted force in the vertical plane during a measurement to ensure the adhesion between end plates and polymer melt.

The prestretch was performed at stretch rates considerably below the inverse of the maximum relaxation time. Subsequently, the samples were allowed to relax until all measurable residual stresses in the polymer had disappeared. SEC was applied on all samples after an elongational experiment to check that no degradation of the polystyrene had occurred during the experiment.

In start-up of elongational flow, the sample is at rest for $t < 0$, while a constant elongation rate $\dot{\epsilon}_0$ is applied for $t > 0$. To monitor the elongation rate, a Keyence LS7500 laser is used to measure the mid-diameter of the filament during an experiment. The average strain rate, $\dot{\epsilon}_0$, is calculated from the measurement of the diameter by fitting an exponential function $R(t) = R_0 \exp(-\dot{\epsilon}_0 t/2)$, where R_0 is the sample radius at $t = 0$ and $R(t)$ is the measured sample radius at time t. Generally, the relative deviation between measurements and fit never exceeded 0.6%. The only exception is elongation at the highest elongation rates of 0.1 s^{-1}. Here the deviation was within 2.6%. Hencky strain is defined and calculated as $\epsilon(t) = -2 \ln(R(t)/R_0)$.

The axial force, $F(t)$, is measured using a weight cell mounted on the bottom end plate. This allows the calculation of the transient elongational viscosity $\bar{\eta}^+(t)$ as

$$\bar{\eta}^+(t) = \frac{\sigma_{zz} - \sigma_{rr}}{\dot{\epsilon}_0} = \frac{F(t) - m_f g/2}{\pi R(t)^2 \dot{\epsilon}_0} \tag{5}$$

where g is the gravitational acceleration, m_f is the weight of the

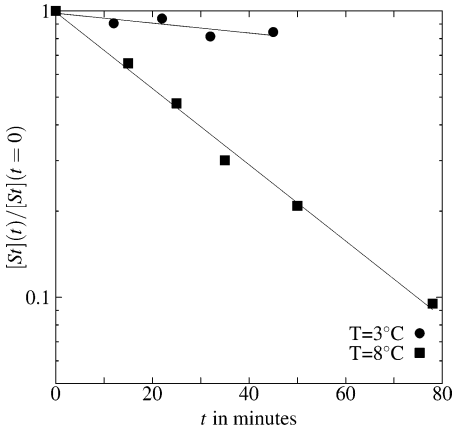

Figure 4. Relative styrene concentration, [St](t)/[St](t=0), at temperatures T = 3 °C and T = 8 °C, as a function of the time, t, in a 3% THF solution.

polymer filament,[17] and $\sigma_{zz} - \sigma_{rr}$ is the stress difference between the axial and radial component of the stress tensor.

At small strains there are an extra force contribution from the shear components in the deformation field during start-up. For Newtonian fluids this reverse squeeze flow problem can be modeled analytically, and the effect of the additional shear may be eliminated by a correction factor[18] to yield for the corrected transient uniaxial elongation viscosity and ϵ_0:

$$\bar{\eta}^{+}_{\mathrm{corr}} = \bar{\eta}^{+}\left(1 + \frac{\exp(-7(\epsilon + \epsilon_0)/3)}{3\Lambda_i^{\,2}}\right)^{-1} \tag{6}$$

Here $\Lambda_i = L_i/R_i$ is the aspect ratio computed from the initial sample length L_i and radius R_i prior to prestretching while $\epsilon_0 = 2\ln(R_i/R_0)$ is the Hencky strain of the prestretched configuration. This correction is analytically correct for very small strains for all types of fluids. However, the correction is less accurate at increasing strains where the effect of the correction fortunately vanishes.[19] In the following we show both uncorrected and corrected data. For the aspect ratios used here, the extra force contribution is negligible (less than 10%) after less than 0.7 strain units of ϵ.

Surface tension has a negligible effect since the viscoelastic surface elasticity number[20] $\sigma/(RG(\dot{\epsilon}_0))$ stays below 0.04 in all experiments. Here σ is the coefficient of surface tension, R is the radius, and $G^* = \sqrt{G'^2+G''^2}$, the complex moduli being evaluated at experimental elongation rates. Likewise, gravity is found to be negligible as the sag time[13] is much longer than the duration of the experiments.

3. Results

3.1. Comparison of Bifunctional Couplers. The results of the two model experiments in which we couple living linear styryl anions with respectively dichlorodimethylsilane and DMDSP are shown in Figure 3. Both DRI signals in the figure have been normalized so that the area under the graphs is unity, and the DRI signal for the DMDSP coupling has been shifted upward with one unit to better distinguish the results. The lengths of styryl anions just prior to coupling are 57.8 kg/mol in the dichlorodimethylsilane experiment and 48.7 kg/mol in the DMDSP experiment, explaining the slight horizontal shift of the peaks for the two experiments.

From the magnitude of the high molecular weight peak compared to the low molecular weight peak, we estimate that the coupling with dichlorodimethylsilane gives a yield of about 40%, whereas the yield using DMDSP is 60%. Hence, we use DMDSP as coupler for the pom-pom synthesis.

3.2. Kinetics Experiment. Figure 4 shows the styrene monomer concentration at 3 and 8 °C as a function of the time in a 3 wt % THF solution in cyclohexane. The measurements confirm that the reaction is first order in the concentration of styrene monomer [St](t) so the concentration decreases according to [St](t)/[St](t=0) = $\exp(-k(T)t)$. Moreover, from the kinetics we expect the temperature-dependent rate constant $k(T) \propto \sqrt{[\mathrm{BuLi}]}$, where [BuLi] is the initial concentration of *sec*-butyllithium.

The presence of THF increases the reaction rate considerably. The values of $k(T)$ at 3 and 8 °C is 0.0040 and 0.031 min^{-1}, respectively. At the temperature of 8 °C the reaction rate turned out to be similar to ordinary anionic polymerization of linear polystyrenes in pure cyclohexane performed at room temperature. Therefore, the polymerizations of the pom-pom and asymmetric star were performed at 8 °C. The estimated reaction time for 95% conversion of the styrene at 8 °C becomes $-\ln(0.05)/(0.031\ \mathrm{min}^{-1}) \approx 100$ min. We use this estimate to determine the optimal time for addition of DMDSP (coupling for pom-pom synthesis) or methanol (for termination of asymmetric star).

3.3. Molecular Structure. The relation between the retention volume, RV, in the SEC measurements and molar mass, M, is based on calibration with linear polystyrene. In the range of molar masses investigated the calibration curve is given to sufficient accuracy by the relation $\log M(RV) = a_0 + a_1 RV$, where a_0 and a_1 are constants ($a_1 < 0$) independent of M. Moreover, let the molar mass change from M to $M + \mathrm{d}M$ when the retention volume changes from RV to $RV + \mathrm{d}RV$. Since the DRI signal is proportional to the mass concentration, we then have

$$P(M)M\,\mathrm{d}M = kDRI(RV)\,\mathrm{d}RV \tag{7}$$

where $P(M)$ is the molar mass distribution function and k is a constant independent of molar mass. It follows that

$$P(M) = k\frac{DRI(RV)}{M}\frac{\mathrm{d}RV}{\mathrm{d}M} = \bar{k}\frac{DRI(RV)}{M^2} \tag{8}$$

Equation 8 also allows the inverse calculation from the distribution function to a DRI signal.

While anionic polymerization under ideal conditions would result in a Poisson distribution of very narrow MMD,[21] nonideal conditions will inevitably result in broader MMD than predicted by the Poisson distribution. To model the data, we choose a Schultz−Zimm distribution[22−24] in the form

$$P_n(M) = \frac{M^{n\mu-1}\exp(-M/\alpha)}{\Gamma(n\mu)\alpha^{n\mu}} \tag{9}$$

Here Γ is the Gamma function and $n \geq 1$ denotes the number of arms in the stars, with $n = 1$ corresponding to the initial chains. The molar mass distribution for the initial arms is described by $n = 1$. The distribution in eq 9 then gives $M_{\mathrm{n,A}} = \alpha\mu$ and $M_{\mathrm{w,A}}/M_{\mathrm{n,A}} - 1 = 1/\mu$. The two free parameters α and μ are therefore determined from the SEC data for the initial chains (A) by substituting the measured number- and weight-average molar mass into these relations with the results in Table 2. The SEC output for the initial chains appears together with the resulting Schultz−Zimm distribution (recalculated to a DRI signal) in Figure 5. Note the small peak of about twice the molar mass. This is the result of termination of living anions due to the presence of oxygen in the syringe used for sample takeout.

Based on the assumption of an ideal reaction kinetics in the linking of the chains (A), the distribution function, P_n, of the n-armed stars may be computed from successive convolution

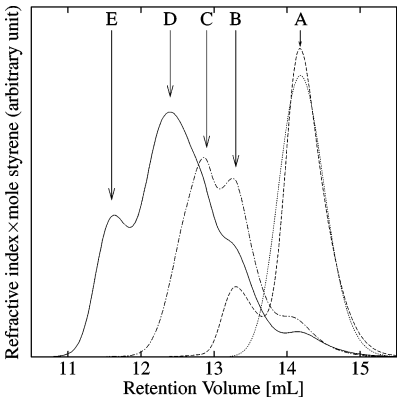

Figure 5. SEC chromatograms for the individual steps in the "pom-pom" synthesis. The refractive index (DRI) signals are normalized with the area beneath the curve and subsequently multiplied by the total amount of added moles of styrene in the reaction mixture. The dashed (− − −), dotted/dashed (− · −), and solid (—) lines are the reaction bath after the first, second, and fourth step as described in sections 2.3 and 2.4. (A) Initial chain (arms); (B) dimers; (C) stars; (D) star-*block*-linear or "asymmetric star"; (E) "pom-pom" molecule. The dotted line is the Schultz−Zimm distribution in eq 9 with $n = 1$, $M_{n,A} = 28$ kg/mol, and $M_{w,A}/M_{n,A-1} - 1 = 0.06$ recalculated to a DRI signal.

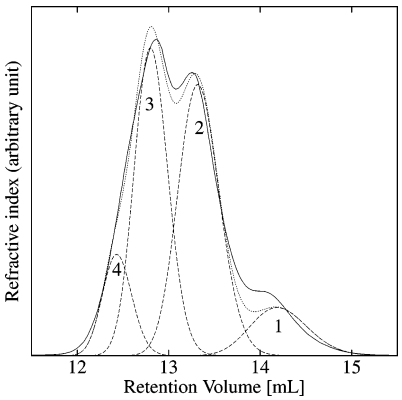

Figure 6. SEC chromatogram for the intermediate stars (A_n). The solid line (—) shows the measured DRI signal for the intermediate star (A_n) molecules in the "pom-pom" synthesis. This correspond to the dotted/dashed line in Figure 5. The measured DRI signal is shown together with a least-squares fitting based on the overall $P(M)$ (dotted line, ···) and individual distribution functions $P_n(M)$, $n = 1$, 2, 3, and 4, from eq 11 (dashed lines, − − −). All molar masses are recalculated to a DRI signal based on calibration with linear polystyrene.

integrals.[11] The distribution in eq 9 is adjusted so the convolution is performed simply by adding indices

$$P_{n+m}(M) = \int_0^M P_n(M_1)\, P_m(M - M_1)\, \mathrm{d}M_1 \qquad (10)$$

where $P_{n+m}(M)$ is given again by eq 9. The predicted number- and mass-average molar mass of the A star is then given by $M_{n,A_n} = n\alpha\mu$ and $M_{w,A_n}/M_{n,A_n} - 1 = 1/(n\mu)$, respectively.

It remains to determine the distribution of arms in the stars. While ideal reaction kinetics may suggest a Poisson distribution, we choose to determine the relative amounts from the SEC data. In so doing, we make use of the observation[25] that retention volume of polystyrene stars with up to four arms is approximated by that of linear polystyrene of the same molar mass. Moreover, we use an overall distribution function of

$$P(M) = \sum_{n=1}^{4} p_n P_n(M) \qquad (11)$$

where the p_n are free parameters. Figure 6 shows the DRI signal for the intermediate star (A_n) molecules (solid line) in the pom-pom synthesis. The measured DRI signal is shown together with the overall $P(M)$ (dotted line) and individual distribution functions $p_n P_n(M)$, $n = 1$, 2, 3, 4 (dashed lines), for the parameter combination $(p_1, p_2, p_3, p_4) = (0.220, 0.445, 0.276, 0.059)$ obtained from a least-squares fitting. However, not all stars are chemically active. In particular, it may be seen from Figure 5 that a fraction of the single arms do not react further. If we assume that all single arms are inactive, the number-average $N_n = 2.5$. We point out that a Poisson distribution

$$n_i = (N_n - 1)^{i-1} \exp(1 - N_n)/(i - 1)! \qquad (12)$$

with number-average $N_n = 2.5$ would give $(n_1, n_2, n_3, n_4, ...) = (0.223, 0.335, 0.251, 0.126, ...)$, which is in fact a somewhat broader distribution than that that found by least-squares fitting. In the "asymmetric star" synthesis we obtained a number-average arm number of about $N_n = 3.3$. In both cases the stoichiometry was adjusted so we expected $N_n = 3$.

Figure 7 shows the distribution function, $P(M)$, as a function of the molecular weight, M, calculated using eq 8 (based on the calibration with linear polystyrenes), of the final reaction mixture of the pom-pom molecule after five fraction steps. The final value of M_w/M_n was estimated to be 1.08 for both the pom-pom and asymmetric star. These polydispersities were based on the SEC calibration with linear polystyrenes. The fractioned pom-pom mixture contains almost no fractions of linear arms and stars and only a minor fraction of "asymmetric stars". The amount of low molecular weight byproducts left, mainly "asymmetric star" molecules, can be estimated to be about 7 wt % using the distribution function in Figure 7. The fractionation of the "asymmetric star" molecule required only three fractionation steps to obtain a final value of M_w/M_n of 1.08.

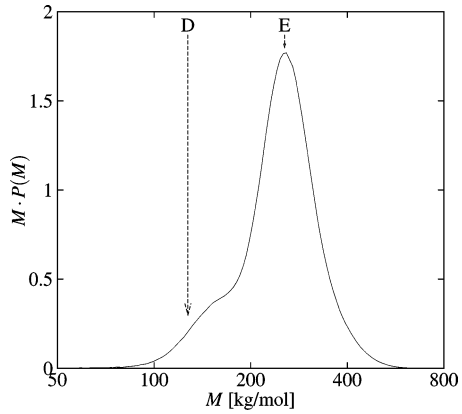

Figure 7. Molecular weight distribution after four fractionation steps in the pom-pom reaction batch. The calculated distribution function, $P(M)$, is shown as a function of the molecular weight, M, using eq 8 based on the calibration with linear polystyrenes. (D) corresponds to M_n of the star-block-linear or "asymmetric star" and (E) the M_n of the "pom-pom" molecule.

The M_w obtained from the calibration curve with linear standards (280 kg/mol) is about 7% smaller than that obtained from eq 3 (300 kg/mol). While this is qualitatively in agreement with expectations for branched polymers, the difference is in fact within experimental error. This may be due to the relatively low degree of branching in the molecules.[25] Based on number averages, the molar mass in the cross-bar is obtained by subtracting the arms from the total mass.

3.4. Linear Rheology. We analyze the LVE data with a theoretical approach suggested by Jackson and Winter[26] which handles mono- and bidisperse linear polymer melts using the

BSW model.[27] Given the separation of time scales into arm dynamics and cross-bar dynamics, we propose to model the relaxation modulus by a double-mode BSW model. In terms of the continuous relaxation spectrum $H_i(\lambda)$,[15] we then use

$$G(t) = \sum_{i=1}^{2} G_i(t) \tag{13}$$

$$G_i(t) = \int_0^\infty \frac{H_i(\lambda)}{\lambda} \exp(-t/\lambda)\, d\lambda, \quad i = 1,2 \tag{14}$$

$$H_i(\lambda) = n_e G^0_{N,i}\left[\left(\frac{\lambda}{\lambda_{\max,i}}\right)^{n_e} + \left(\frac{\lambda}{\lambda_c}\right)^{-n_g}\right] h(1 - \lambda/\lambda_{\max,i}), \quad i = 1,2 \tag{15}$$

Here $h(x)$ is the Heaviside step function. In the absence of glassy modes the parameter n_e is the absolute value of the slope of $\log(G'')$ as a function of $\log(\omega)$ for both contributions to G'', while n_g is the slope of $\log(G'')$ as a function of $\log(\omega)$ in the glassy region for high ω. The parameter λ_c, called the crossover relaxation time, depends on temperature as any other relaxation time while n_e and n_g are independent of temperature. The plateau modulus, obtained as $G^0_N = G^0_{N,1} + G^0_{N,2}$, corresponds to $G(0)$ where the glassy part of the spectrum has been excluded. This definition of the plateau modulus is then the elastic modulus in fast deformation of the hypothetical material in which the glassy behavior is neglected. Our expression is in agreement with the integral involving the loss modulus given in ref 15, the two expressions being related by a Fourier transformation. However, in practice, the methods differ in the way the glassy behavior is filtered out.

The constants $n_g = 0.67$ and $\lambda_c = 0.4$s (at $T = 130$ °C), as obtained from Jackson and Winter.[26] The remaining parameters have been adjusted by least-squares fitting to G' and G'' data.[28] The resulting parameters are given in Table 2. Also included in the table are the LVE properties of a linear polystyrene of molar mass 390 kg/mol.[14]

On the basis of the parameters in Table 2, we define Deborah numbers as

$$De_i = \dot{\epsilon}_0 \lambda_{a,i} \approx \dot{\epsilon}_0 \lambda_{\max,i} \frac{1 + n_e}{2 + n_e} \tag{16}$$

where $\lambda_{a,i}$ is defined as

$$\lambda_{a,i} = \frac{\int_0^\infty G_i(s) s\, ds}{\int_0^\infty G_i(s)\, ds} \tag{17}$$

For the pom-pom polystyrene, De_1 is a Deborah number for cross-bar relaxation, while De_2 is a Deborah number for arm relaxation. The rationale behind the definition in eq 17 is that for a linear polymer this definition gives a value that is within a few percent of the Doi−Edwards reptation time, τ_d.

3.5. Start-Up of Elongational Flow. Figures 10 and 11 show the measured corrected transient elongational viscosity $\bar{\eta}^+_{corr}(t)$ for the pom-pom and asymmetric star molecule along with predictions from LVE at 130 °C. The elongational viscosity measurements rates were performed at 130 °C, except for the two lowest elongational rates for the pom-pom molecule. They were measured at 150 °C, and then subsequent time−temperature superposition shifted to 130 °C. The LVE predictions were based on the parameters in Table 2. In both plots there is agreement between measurements and LVE predictions up to a certain level of strain. It is seen that the transient elongational viscosity rises above LVE at intermediate strains. Note that the transient elongational viscosity for the pom-pom melt exhibits a maximum as a function of time for $\dot{\epsilon} = 0.1$ s^{-1}. Such a maximum has been observed previously in branched polymer melts (low-density polyethylene)[7,29] but to our knowledge not in a well-characterized material. We show a second independent experiment in Figure 13, where we use a linear scale for the stress difference, that also shows the maximum. Generally all data points in Figures 10 and 11 have been reproduced within a 15% scattering The maximum appears when the arm Deborah number $De_2 > 1$, whereas $\bar{\eta}^+(t)$ is monotone, increasing for $De_2 < 1$. While a simple explanation for the maximum has been proposed elsewhere,[7] we do not pursue mechanism further here.

As an alternative representation, we plot the same data as uncorrected stress vs strain in Figures 13 and 14. In this representation the duration of the steady-state elongational viscosity is more apparent. The elongational viscosity for the pom-pom molecule reaches a steady state in all series except at the highest elongational rate. Here the elongational viscosity does not reach a steady plateau at high strain but is going

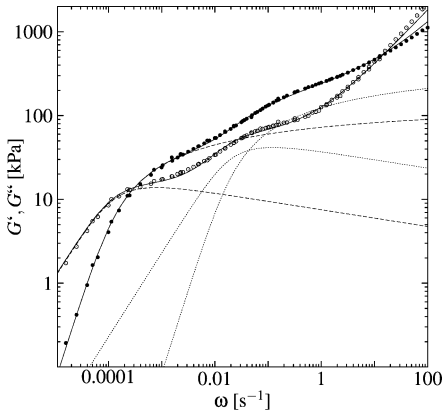

Figure 8. Linear viscoelastic data for the pom-pom polystyrene melt. The measurements were performed at 130, 140, 150, and 170 °C. The data are all time−temperature shifted to 130 °C. Open circles (○) are the loss modulus (G'') and bullets (●) the storage modulus (G'), both as a function of the angular frequency, ω. The solid lines (—) are the least-squares fitting to the BSW model in eqs 13−15. The dashed lines (− − −) and dotted lines (···) are the first and second rubbery mode in the fitted BSW model.

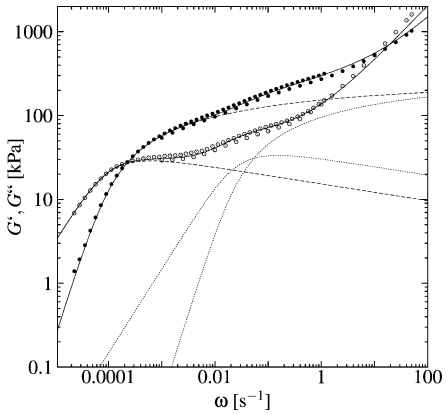

Figure 9. Linear viscoelastic data for the "asymmetric star" polystyrene melt. The measurements were performed at 130 and 150 °C. The data are all time−temperature shifted to 130 °C. Open circles (○) are the loss modulus (G'') and bullets (●) the storage modulus (G'), both as a function of the angular frequency, ω. The solid lines (—) are the least-squares fitting to the BSWmodel in eqs 13−15. The dashed lines (− − −) and dotted lines (···) are the first and second rubbery mode in the fitted BSW model.

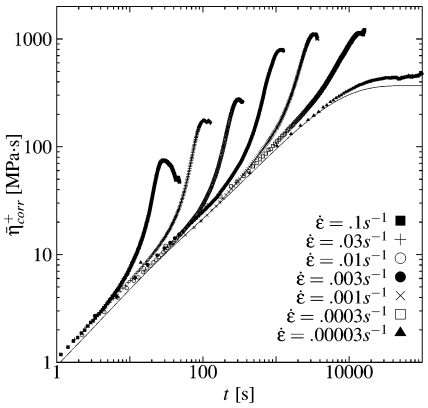

Figure 10. Corrected transient elongation viscosities $\bar{\eta}^+_{corr}$ of the pom-pom melt at 130 °C, using eq 6, shown as a function of the time, t. The line is the linear viscoelastic prediction of the transient elongational viscosity. $\bar{\eta}^+_{corr}$ was measured at seven different elongational rates $\dot{\epsilon}$ (shifted to 130 °C) of 0.1, 0.03, 0.01, 0.003, 0.001, 0.0003, and 0.00003 s^{-1} as shown in the figure.

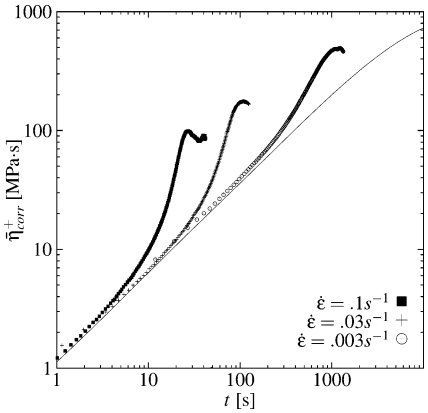

Figure 11. Corrected transient elongation viscosities $\bar{\eta}^+_{corr}$ corr of the "asymmetric star" melt at 130 °C, using eq 6, shown as a function of the time, t. The line is the linear viscoelastic prediction of the transient elongational viscosity. $\bar{\eta}^+_{corr}$ was measured at three different elongational rates $\dot{\epsilon}$ of 0.1, 0.03, and 0.003 s^{-1} as shown in the figure.

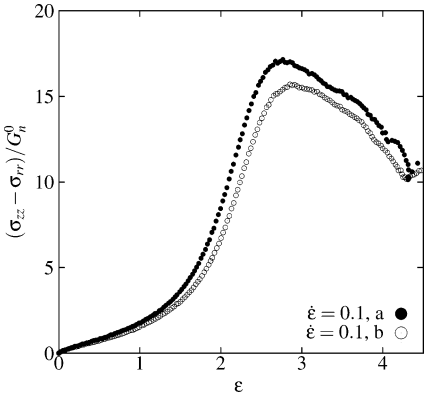

Figure 12. Uncorrected stress difference $\sigma_{zz} - \sigma_{rr}$ (eq 5) relative to the elastic modulus, G^0_N, as a function of the Hencky strain, ϵ, for the pom-pom melt for two experiments at $\dot{\epsilon} = 0.1$ s^{-1} measured at 130 °C. The stress goes through a reproducible maximum whereafter it decays about 30%. No steady stress is observed.

through a significant maximum in the transient elongational viscosity. Apart form this experiment, the plateau values of stress are constant within 10% for (at least) one strain units, except at the fastest (0.1 s^{-1}) measurement on the "asymmetric star" molecule where the deviation is 20%. The fluctuations in the steady-state value are correlated with small changes in the instantaneous strain rate.

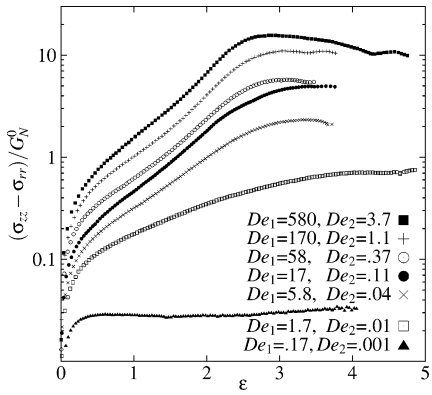

Figure 13. Uncorrected transient stress difference $\sigma_{zz} - \sigma_{rr}$ relative to the elastic modulus, G^0_N, of the pom-pom melt using eq 5, shown as a function of the Hencky strain, ϵ. The stress differences were measured at 130 and at 150 °C for the two lowest elongational rates. The measurements at 150 °C were time−temperature superposition shifted to 130 °C.

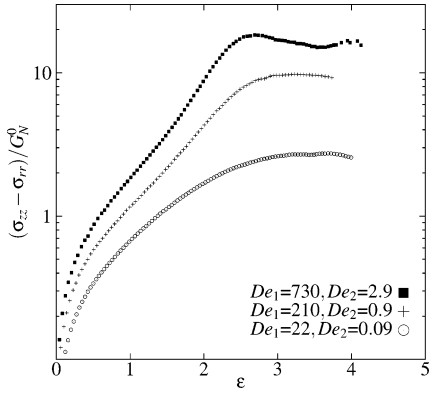

Figure 14. Uncorrected transient stress difference $\sigma_{zz} - \sigma_{rr}$ relative to the elastic modulus, G^0_N, of the "asymmetric star" melt measured at 130 °C, using eq 5, and shown as a function of the Hencky strain, ϵ.

4. Discussion

A key issue in the constitutive modeling of polymeric liquids is the factorization of the kernel functions in integral models into a product of time-dependent and strain-dependent factors.[30,31] While such a factorization is assumed in the theory of linear viscoelasticity and almost universally observed for small deformations, the situation is more open for large deformations. By way of examples, the now classical pom-pom model[5] for branched polymer melts is not separable in time and strain, whereas the molecular stress function (MSF)[32] model is. Moreover, whereas the strain and time contributions to stress are straightforward to uncouple in step strain experiments, the two contributions are convoluted in start-up of flow. However, in an early investigation on branched polyethylene, Wagner[8] devised a method to deconvolute the contributions. Following that method we consider a generic time−strain separable integral constitutive for which the stress in elongational flow is given by

$$\sigma(t) = \sigma_{zz} - \sigma_{xx} = \int_{t'=-\infty}^{t} M(t - t')\, S(\epsilon(t, t'))\, \mathrm{d}t' \quad (18)$$

Here $M(s)$ is the time-dependent memory function, and σ_{zz} and σ_{xx} are respectively the axial and transverse components of stress tensor. Likewise, S is the difference between the zz and xx

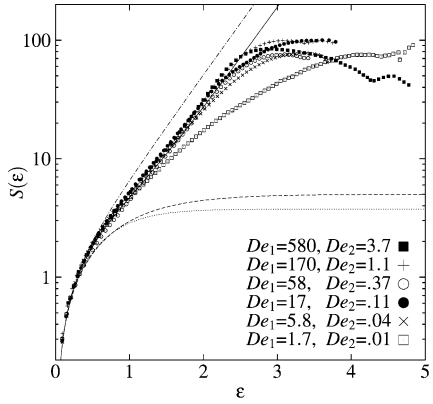

Figure 15. Strain function, $S(\epsilon)$ defined in eq 18, as computed from eq 22 for pom-pom polystyrene. The figure is based on the (corrected) viscosity measurements in Figure 10 measured at 130 °C. Except for $De_1 = 1.7$, the data do show a unique function $S(\epsilon)$. The full line is the prediction of H-polymer theory (eq 33) with $\phi_a = 0.50$ and $\phi_b = 0.50$. The dashed−dotted line is eq 29. The lower dashed and dotted lines are eqs 34 and 32, respectively.

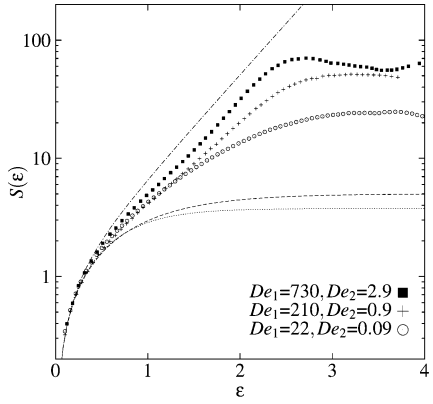

Figure 16. Attempt to compute the strain function, $S(\epsilon)$, defined in eq 18, from eq 22 for asymmetric star polystyrene. The data do not show a unique $S(\epsilon)$. The figure is based on the (corrected) viscosity measurements in Figure 11 measured at 130 °C. The dashed−dotted line is eq 31. The lower dashed and dotted curves are eqs 34 and 32, respectively.

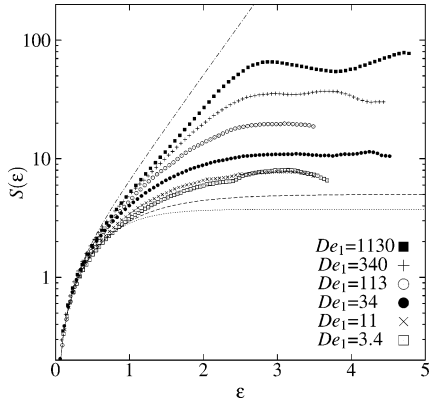

Figure 17. Attempt to compute the strain function, $S(\epsilon)$, defined in eq 18, from eq 22 for narrow molar mass distribution linear polystyrene melt with a molar mass of 390 kg/mol. The data do not show a unique $S(\epsilon)$. The figure is based on the time-dependent elongational viscosity measurements of Bach et al.[16] (Figure 6). The dashed−dotted line is eq 31. The lower dashed and dotted curves are eqs 34 and 32, respectively.

component of the nonlinear strain measure which again is a function of the Hencky strain:

$$\epsilon(t, t') = \begin{cases} \dot{\epsilon}_0 t, & t' < 0 \\ \dot{\epsilon}_0 (t - t'), & t' > 0 \end{cases} \tag{19}$$

Hence

$$\sigma(t) = G(t) S(\dot{\epsilon}_0 t) + \int_{s=0}^{t} M(s)\, S(\dot{\epsilon}_0 t)\, \mathrm{d}s \tag{20}$$

This equation may be solved for S to yield

$$\frac{\mathrm{d}}{\mathrm{d}t} S(\dot{\epsilon}_0 t) = \frac{1}{G(t)} \frac{\mathrm{d}\sigma}{\mathrm{d}t} \tag{21}$$

where $G(t)$ is the relaxation modulus related to the memory function by $M(s) = -\mathrm{d}G(s)/\mathrm{d}s$. An integration by parts then yields the Wagner[8] expression for the strain measure:

$$S(\epsilon) = \frac{\sigma(t)}{G(t)} - \int_0^t \frac{M(t')}{(G(t'))^2} \sigma(t')\, \mathrm{d}t' \tag{22}$$

where $\epsilon = \dot{\epsilon}_0 t$. In other words, if the assumption of time−strain factorability holds, then the above expression should give a unique function $S(\epsilon)$ independent of the applied strain rate $\dot{\epsilon}_0$.

In the application of this formula we use the corrected stress values from eq 6. As mentioned, this correction is analytically correct for very small strains, but less accurate and tending to zero at increasing strains. The result of eq 22 for $S(\epsilon)$ is shown in Figures 15 and 16, using the measurements from Figures 10 and 11, respectively. We also include a figure with the elongational-based strain function for a narrow MMD linear polystyrene with a molar mass of 390 kg/mol in Figure 17. That strain function is calculated using the LVE and elongational measurements from Bach et al.[16] The transient and steady elongational viscosity, measured on linear monodisperse polystyrenes ranging from a molecular weight of 51 to 390 kg/mol,[16,33] has been discussed and predicted theoretically recently.[34,35]

We note first of all that for linear polystyrene and for the asymmetric star polystyrene the result of eq 22 is not a function of strain only. This means that the data for linear and asymmetric star polymers melts do not observe time−strain separability in the window of strain rates investigated. Consequently, we must conclude that neither the asymmetric star nor the linear polystyrene melt may be described by a constitutive equation of the generic form in eq 18. On the other hand, for the pom-pom melt, the time−strain separability turns out to be an excellent assumption for almost all investigated rates. Practically all data collapse on a single curve. However, at time scales larger than the reptation time the strain function is significantly lower. This agrees with the observation in ref 2, measuring the nonlinear step shear on a $A_n-C-C-A_n$ pom-pom 1,4-polybutadiene melt, as they observe a transition in the strain curve at the reptation time.

Time−strain separability appears to be connected to the existence of at least two branch points, as neither the "asymmetric star" (Figure 15), containing one branch point, nor the linear molecule (Figure 16) shows any separability. We therefore expect that the separability occurs due to the stretching of the cross-bar between the two branch points.

It is of interest to compare the experimentally observed strain measure with those obtained from the molecular theories for entangled polymer networks without relaxation. We consider a fast deformation in which a given particle with coordinates (x_1', x_2', x_3') in the stress free reference state (time t') is displaced to coordinates (x_1, x_2, x_3) in the current state (time t). Then the

components macroscopic displacement gradient tensor is given by

$$E_{ij}(x,t,t') = \frac{\partial x_i}{\partial x_j}, \quad i = 1, 2, 3 \text{ and } j = 1, 2, 3 \tag{23}$$

A tube segment of unit length and orientation given by the unit vector **u** in the stress free state is deformed into **E·u** in the current state. The tube model for an entangled network[36] then gives the following expression for the free energy in the deformed state:

$$A(\mathbf{E}) = \frac{3}{2} n_c k_B T \frac{Z^2 a^2}{Nb^2} \langle |\mathbf{E}\cdot\mathbf{u}|^2 \rangle$$

$$= \frac{3}{2} n_c k_B T Z \langle |\mathbf{E}\cdot\mathbf{u}|^2 \rangle \tag{24}$$

Here n_c is the number density of chains, k_B Boltzmann's constant, T the absolute temperature, N the number of Kuhn steps in the chain, b the Kuhn step length, a the tube diameter, and Z the number of entanglements per chain, and we have used that $Za^2 = Nb^2$. The angular brackets denote an average over a unit sphere:

$$\langle \cdots \rangle = \frac{1}{4\pi} \int_{|\mathbf{u}|=1} \cdots \, \mathrm{d}\mathbf{u} \tag{25}$$

Basically $|\mathbf{E}\cdot\mathbf{u}|$ is the stretch factor for a tube segment. The corresponding stress tensor may found by computing the time derivative of A

$$\frac{\mathrm{d}}{\mathrm{d}t} A = \frac{\partial A}{\partial E_{jn}} \frac{E_{jn}}{\partial t} \tag{26}$$

$$= \frac{\partial A}{\partial E_{jn}} E_{in} (\nabla v)_{ij} \tag{27}$$

where $(\nabla v)_{ij}$ are the components of the velocity gradient. By comparing this result with the rate of doing work, it follows that apart from an additive isotropic pressure the stress tensor components must be given by

$$\sigma_{ij} = \frac{\partial A}{\partial E_{jn}} E_{in} \tag{28}$$

In particular, for the expression in eq 24

$$\sigma_{ij} = 3 n_c k_B T Z \langle |\mathbf{E}\cdot\mathbf{u}| \rangle \left\langle \frac{E_{in} u_n E_{jm} u_m}{|\mathbf{E}\cdot\mathbf{u}|} \right\rangle \tag{29}$$

$$= n_c k_B T Z \left(\delta_{ij} + \frac{4}{5} (\alpha_{ij} + \alpha_{ji}) + \ldots \right) \tag{30}$$

In the second line we have specialized to small deformation in which $E_{ij} = \delta_{ij} + \alpha_{ij}$, where δ_{ij} is Kroneckers delta and α_{ij} is the infinitesimal deformation gradient. Hence the factor in front of the infinitesimal strain tensor must be the elastic modulus of the network, $G = (4/5) n_c k_B T Z = (4/5) \rho RT / M_e$, where ρ is the density and M_e the molar mass between entanglements. With this definition of G, eq 29 may be written in the form

$$\sigma_{ij}^{\mathrm{NET}} / G = \frac{15}{4} \langle |\mathbf{E}\cdot\mathbf{u}| \rangle \left\langle \frac{E_{in} u_n E_{jm} u_m}{|\mathbf{E}\cdot\mathbf{u}|} \right\rangle \tag{31}$$

The decoration NET has been added to indicate an entanglement network without chain retraction. The corresponding strain measure is therefore the expression on the right of eq 31. Conversely, the Doi−Edwards strain measure for an entanglement network with instantaneous chain retraction becomes

$$\sigma_{ij}^{\mathrm{DE}} / G = \frac{15}{4} \frac{1}{\langle |\mathbf{E}\cdot\mathbf{u}| \rangle} \left\langle \frac{E_{in} u_n E_{jm} u_m}{|\mathbf{E}\cdot\mathbf{u}|} \right\rangle \tag{32}$$

We are now in a position to test the assumption that the pom-pom cross-bar is unrelaxed while the arms are fully relaxed. The corresponding stress would then be

$$\sigma_{ij}^{\mathrm{H}} = \phi_b \sigma_{ij}^{\mathrm{NET}} + \phi_a \sigma_{ij}^{\mathrm{DE}} \tag{33}$$

as predicted by H-polymer theory.[1] Here the ϕ_b and ϕ_a are the volume fractions of cross-bar and arms, respectively. The expression is expected to hold until branch-point withdrawal occurs.

For completeness we give the corresponding expression for the Doi−Edwards model[37,38] with the independent alignment approximation included:

$$\sigma_{ij}^{\mathrm{IIA}} / G = 5 \left\langle \frac{E_{in} u_n E_{jm} u_m}{|\mathbf{E}\cdot\mathbf{u}|^2} \right\rangle \tag{34}$$

All of the above strain measures have the property of simplifying to the infinitesimal strain tensor for small deformations.

We have included a number of the above predictions in Figures 15−17 although the comparison is meaningful for the pom-pom melt only.

For the pom-pom melt, where we do get a unique function $S(\epsilon)$, it appears that the data are well described by the H-polymer model in eq 33 up to a total Hencky strain of about 2.6. In other words, the data support an interpretation that there is no relaxation in the cross-bar tube while the arms are fully retracted to their equilibrium length in their short tubes of merely two entanglements.

The critical Hencky strain that we interpret as arm retraction into the cross-bar tube, however, is much larger than the value ($\epsilon_c \approx \ln(\sqrt{3}q) \approx 1.5$ predicted from the force balance argument in H-polymer theory with $q = 2.5$. As an alternative, we estimate the Hencky strain at which the cross-bar on average becomes fully extended. For this purpose we model the cross-bar as a Kramers chain composed of n_K freely jointed Kuhn steps of length l_K. The equilibrium dimension of the chain is then given by $n_K l_K^2 = C_\infty n l^2$, where n is the number of C−C bonds of length l and $C_\infty = 9.6$ for polystyrene.[39] The maximum chain length is $n_K l_K = 0.83 nl$, where the factor 0.83 is included to take account of the bond angles.[40] We then estimate $n_K = (0.83)^2 n / C_\infty \approx 210$. Hence, the Hencky strain for maximum extension of the cross-bar becomes $\ln(\sqrt{n_K}) \approx 2.7$, which corresponds well with the observed transition to steady stress.

5. Conclusion

We have synthesized two well-characterized model materials for branched polymer melts: one with a single branch point (an asymmetric star) and one with two branch points (a pom-pom). The use of a novel coupler was instrumental in the synthesis.

A filament stretching apparatus was used to measure transient elongational viscosity of the two model branched polymer melts. The transient elongational viscosity for polymer melts without a branch point or with a single branch point is not separable in time and strain. On the other hand, the transient elongational viscosity for the pom-pom melt (two branch points) is separable

in time and strain for times less than the reptation time. We therefore link the separability to the stretching of the cross-bar between two branched points. Moreover, the resulting strain function is well described by a model in which the deformation of the cross-bar is assumed to follow an entanglement network, while the arms are relaxed as in the H-polymer theory.[1] At Hencky strains of about 2.6 a stress saturation occurs that we interpret as withdrawal of the arms into the cross-bar tube. The observed strain associated with arm withdrawal, however, is significantly larger than that predicted from an equilibrium force balance on the branch points while it corresponds well with an estimate of the maximum stretchability of the cross-bar.

Acknowledgment. The authors gratefully acknowledge financial support to the Graduate School of Polymer Science from the Danish Research Training Council and the Danish Technical Research Council to the Danish Polymer Centre. Support from the European Network of Excellence SOFTCOMP is also acknowledged.

References and Notes

(1) McLeish, T. C. B.; Allgaier, J.; Bick, D. K.; Bishko, G.; Biswas, P.; Blackwell, R.; Blottiere, B.; Clarke, N.; Gibbs, B.; Groves, D. J.; Hakiki, A.; Heenan, R. K.; Johnson, J. M.; Kant, R.; Read, D. J.; Young, R. N. *Macromolecules* **1999**, *32*, 6734−6758.
(2) Archer, L. A.; Juliani *Macromolecules* **2004**, *37*, 1076−1088.
(3) Larson, R. G. *Macromolecules* **2001**, *34*, 4556−4571.
(4) Daniels, D. R.; McLeish, T. C. B.; Crosby, B. J.; Young, R. N.; Fernyhough, C. M. *Macromolecules* **2001**, *34*, 7025−7033.
(5) McLeish, T. C. B.; Larson, R. G. *J. Rheol.* **1998**, *42*, 81−110.
(6) Mckinley, G. H.; Hassager, O. *J. Rheol.* **1999**, *43*, 1195−1212.
(7) Rasmussen, H. K.; Nielsen, J. K.; Bach, A.; Hassager, O. *J. Rheol.* **2005**, *49*, 369−381.
(8) Wagner, M. H. *J. Non-Newtonian Fluid Mech.* **1978**, *4*, 39−55.
(9) Knauss, D. M.; Huang, T. *Macromolecules* **2002**, *35*, 2055−2062.
(10) Ndoni, S.; Papadakis, C. M.; Bates, F. S.; Almdal, K. *Rev. Sci. Instrum.* **1995**, *66*, 1090−1095.
(11) Ryu, J.; Im, K.; Yu, W.; Park, J.; Chang, T.; Lee, K.; Choi, N. *Macromolecules* **2004**, *37*, 8805−8807.
(12) Spanggaard, H.; Jørgensen, M.; Almdal, K. *Macromolecules* **2003**, *36*, 1701−1705.
(13) McKinley, G. H.; Sridhar, T. *Annu. Rev. Fluid Mech.* **2002**, *32*, 375−416.
(14) Bach, A.; Rasmussen, H. K.; Hassager, O. *J. Rheol.* **2003**, *47*, 429−441.
(15) Ferry, J. *Viscoelastic Properties of Polymers*; Wiley: New York, 1980.
(16) Bach, A.; Almdal, K.; Rasmussen, H. K.; Hassager, O. *Macromolecules* **2003**, *36*, 5174−5179.
(17) Szabo, P. *Rheol. Acta* **1997**, *36*, 277−284.
(18) Spiegelberg, S. H.; McKinley, G. H. *J. Non-Newtonian Fluid Mech.* **1996**, *64*, 229−267.
(19) Kolte, M. I.; Rasmussen, H. K.; Hassager, O. *Rheol. Acta* **1997**, *36*, 285−302.
(20) Eriksson, T.; Rasmussen, H. K. *J. Non-Newtonian Fluid Mech.* **2005**, *127*, 191−200.
(21) Flory, P. J. *Polymer Chemistry*; Cornell University Press: Ithaca, NY. 1969; p 337.
(22) Almdal, K. In *Developments in Block Copolymer Science and Technology*; Hamley, I. W., Ed.; John Wiley & Sons: New York, 2004; pp 31−69.
(23) Schulz, G. V. *Z. Phys. Chem. B* **1939**, *43*, 25−46.
(24) Zimm, B. H. *J. Chem. Phys.* **1948**, *16*, 1093−1099.
(25) Jankova, K.; Bednarek, M.; Hvilsted, S. *J. Polym. Sci., Part A: Polym. Chem.* **2005**, *43*, 3748−3759.
(26) Jackson, J. K.; Winter, H. H. *Macromolecules* **1996**, *28*, 3146−3155.
(27) Baumgaertel, M.; Schausberger, C.; Winter, H. H. *Rheol. Acta* **1990**, *29*, 400−408.
(28) Rasmussen, H. K.; Christensen, J. H.; Gottsche, S. J. *J. Non-Newtonian Fluid Mech.* **2000**, *93*, 245−263.
(29) Meissner, J. *Chem. Eng. Commun.* **1985**, *33*, 159−180.
(30) Bird, R. B.; Armstrong, R. C.; Hassager, O. *Dynamics of Polymeric Liquids*, 2nd ed.; Wiley: New York, 1987; Vol. 1.
(31) Larson, R. G. *Constitutive Equations for Polymer Melts and Solutions*; Butterworth: Guilford, 1988.
(32) Wagner, M. H.; Rubio, P.; Bastian, H. *J. Rheol.* **2001**, *45*, 1387−1412.
(33) Nielsen, J. K.; Rasmussen, H. K.; Hassager, O.; McKinley, G. H. *J. Rheol.* **2006**, *50*, 453−476.
(34) Marrucci, G.; Ianniruberto, G. *Macromolecules* **2004**, *37*, 3934−3942.
(35) Wagner, M. H.; Kheirandish, S.; Hassager, O. *J. Rheol.* **2005**, *49*, 1317−1327.
(36) Doi, M. *Introduction to Polymer Pysics*; Oxford University Press: New York, 1997.
(37) Doi, M.; Edwards, S. F. *J. Chem. Soc., Faraday Trans. 2* **1978**, *74*, 1818−1832.
(38) Doi, M.; Edwards, S. F. *J. Chem. Soc., Faraday Trans. 2* **1979**, *75*, 38−54.
(39) Fetters, L. J.; Lohse, D. J.; Richter, D.; Witten, T. A.; Zirkel, A. *Macromolecules* **1994**, *27*, 4639−4647.
(40) Flory, P. J. *Statistical Mechanics of Chain Molecules*; Hanser: Cincinnati, 1989; p 12.

MA061476R